MDPI

Article

QTL Analysis of Five Morpho-Physiological Traits in Bread Wheat Using Two Mapping Populations Derived from Common Parents

Paolo Vitale [1,2,†], **Fabio Fania** [1,†], **Salvatore Esposito** [2], **Ivano Pecorella** [2], **Nicola Pecchioni** [2], **Samuela Palombieri** [3], **Francesco Sestili** [3], **Domenico Lafiandra** [3], **Francesca Taranto** [4,*] and **Pasquale De Vita** [2,*]

1   Department of Agriculture, Food, Natural Science, Engineering, University of Foggia, Via Napoli 25, 71122 Foggia, Italy; paolo.vitale@unifg.it (P.V.); fabio.fania@unifg.it (F.F.)
2   Research Centre for Cereal and Industrial Crops (CREA-CI), CREA—Council for Agricultural Research and Economics, 71122 Foggia, Italy; salvatore.esposito@crea.gov.it (S.E.); ivano.pecorella@crea.gov.it (I.P.); nicola.pecchioni@crea.gov.it (N.P.)
3   Department of Agriculture and Forest Sciences (DAFNE), University of Tuscia, 01100 Viterbo, Italy; palombieri@unitus.it (S.P.); francescosestili@unitus.it (F.S.); lafiandr@unitus.it (D.L.)
4   Institute of Biosciences and Bioresources (CNR-IBBR), 80055 Portici, Italy
*   Correspondence: francesca.taranto@ibbr.cnr.it (F.T.); pasquale.devita@crea.gov.it (P.D.V.)
†   These authors contributed equally to this work.

Abstract: Traits such as plant height (PH), juvenile growth habit (GH), heading date (HD), and tiller number are important for both increasing yield potential and improving crop adaptation to climate change. In the present study, these traits were investigated by using the same bi-parental population at early (F_2 and F_2-derived F_3 families) and late (F_6 and F_7, recombinant inbred lines, RILs) generations to detect quantitative trait loci (QTLs) and search for candidate genes. A total of 176 and 178 lines were genotyped by the wheat Illumina 25K Infinium SNP array. The two genetic maps spanned 2486.97 cM and 3732.84 cM in length, for the F_2 and RILs, respectively. QTLs explaining the highest phenotypic variation were found on chromosomes 2B, 2D, 5A, and 7D for HD and GH, whereas those for PH were found on chromosomes 4B and 4D. Several QTL detected in the early generations (i.e., PH and tiller number) were not detected in the late generations as they were due to dominance effects. Some of the identified QTLs co-mapped to well-known adaptive genes (i.e., *Ppd-1*, *Vrn-1*, and *Rht-1*). Other putative candidate genes were identified for each trait, of which *PINE1* and *PIF4* may be considered new for GH and TTN in wheat. The use of a large F_2 mapping population combined with NGS-based genotyping techniques could improve map resolution and allow closer QTL tagging.

Keywords: bread wheat; SNP markers; genetic map; QTL; RILs; F_2

1. Introduction

Bread wheat (*Triticum aestivum* L.) is grown on more than 200 million hectares of land worldwide, and in 2020, the global production reached about 760 million ton [1]. Despite this, by 2050, wheat production may need to be increased by at least 50% relative to current levels [2,3]. Although crop yields continue to increase globally, climate change represents a tremendous challenge for achieving this objective. In fact, recent research suggests that some major crop yields have already stagnated or even been reduced by the impact of climate change [4]. Phenology genes also regulate the physiological development of wheat [5], and some morpho-physiological traits have been identified as effective in breeding drought-adaptive varieties [6]. Traits such as flowering time, plant height, tiller number, growth habit, flag leaf angle, and spike characteristics, which are important for increasing crop yield potential, are also functional in determining the adaptation of wheat to climate change [7].

Genetic improvement has contributed significantly to modify wheat architecture by reducing plant height through selection of specific alleles at *Rht-1* loci [8] as well as by adjusting flowering time. It is well known that *Ppd* genes influence the plant height, by regulating the number of leaves emitted during the vegetative phase of wheat development, the number of tillers, and fewer spikelets per spike [9]. Giunta et al. [10] demonstrated a major role for the *Vrn* genes on the control of tillering, which was independent of any photoperiod or temperature effects. The wheat ideotype generated during the Green Revolution was also characterized by an erect juvenile growth habit, a reduced number of tillers, and a reduced flag leaf angle [11]. If, on the one hand, this made it possible to increase the investment of plants per unit of area, reducing the intraspecific competition, on the other hand, it made the crop more vulnerable to weeds, reducing interspecific competition. Unfortunately, the trade-off between productivity in weed-free situations and competitive ability is a main obstacle to the release of competitive cultivars [7]. Genetic linkage mapping in segregating populations is one of the traditional approaches to gain insights into the genetic control of key characteristics using quantitative trait locus (QTL) analysis and is a suitable method underlying the molecular marker-assisted selection (MAS) in wheat [12]. The commonly used mapping populations in plants include F_2, backcross (BC), double haploid (DH), and recombinant inbred line (RIL) populations [13,14]. Among these, the F_2 population, using codominant markers, provides the most abundant genetic information, including effects such as epistasis and dominance [15]. Ferreira et al. [16], in a simulation study, showed that more accurate maps were obtained with F_2 codominant and RILs than with BC, DH, and F_2-dominant populations.

Several studies have been successfully conducted using F_2 or F_2-derived F_3 populations to identify major QTLs in bread wheat [17–19], durum wheat [20], rice [21], maize [22], and other species [23–26]. However, unfortunately, F_2 and BC are temporary populations. To analyze QTL × E interactions it is necessary to employ permanent populations such as DHs and RILs that can be maintained under several experimental conditions [14].

The RIL populations have several advantages for use in QTL mapping, which have been described by several authors [27–30]. Multiple selfing processes can increase the number of recombination events [31], which results in a finer mapping of QTLs, but the most important aspect is that once RILs are established they can be repeatedly used for investigating the QTLs of various phenotypes under different environments [10]. However, at least six generations are required to obtain the RILs and they are not suitable to estimate dominance effects of mapped QTLs due to the absence of heterozygous genotypes [32]. Nonetheless, RILs have been extensively used in wheat to identify QTLs for yield [33,34] and other important agronomic traits such as plant height [35], flowering time [36–38], and tiller number [39–43]. Otherwise, studies conducted for mapping the juvenile growth habit have been very limited [44].

The knowledge previously acquired by using bi-parental populations and the current availability of high-throughput and cost-effective single nucleotide polymorphism (SNP) genotyping platforms have opened the way for understanding the genetic mechanisms of these important agronomic traits [45].

Stable QTLs are a prerequisite for their use in a marker-assisted breeding program. To validate the QTLs, it is necessary to confirm them in other mapping populations, or in different generations from the same crossing, or using the same RIL population evaluated in multiple locations and in multiple years [46]. QTLs with large effects should be detected consistently across generations, but the increased precision of the RILs should allow the detection of QTLs with smaller effects [16]. In addition, additional opportunities for recombination should improve the genetic resolution of linked QTLs and distinguish linked effects from pleiotropic ones in some instances [47].

In this study, we performed QTL analysis of five morpho-physiological traits, all potentially associated with the yield potential and adaptability in bread wheat, using the same bi-parental population at early (F_2 and F_2-derived F_3) and late (RIL F_6 and F_7) stages of inbreeding. We aimed to improve the understanding of the genetic basis (including additive and dominance effect) by comparing the QTLs detected by both populations, which were grown at the same location and evaluated in two years each. In addition, based on a priori knowledge of genes with biological function regulating the investigated traits in wheat and in other species, we also searched for putative candidate genes in chromosome regions tightly linked to QTLs for those traits by exploiting the reference bread wheat genome.

2. Materials and Methods

2.1. Plant Material and Field Trials

Two mapping populations derived from common parents, Lankaodali and Rebelde, were developed at the Department of Agriculture and Forest Sciences, University of Tuscia, Viterbo, Italy, in collaboration with the CREA Research Centre for Cereal and Industrial Crops (CREA-CI), Foggia, Italy. The female parent, Lankaodali, is a Chinese bread wheat cultivar with very large kernels [48], low tillering capacity, and a medium flowering time. The male parent, Rebelde (Bologna/CH-710//Bologna), is an Italian hard winter wheat cultivar with excellent agronomic characteristics, medium-late flowering time, and high tillering capacity. The two cultivars were crossed for generating first an F_2 population; then, by advancing through single seed descent, a F_6 RIL population was generated.

A total of 176 F_2 individual plants and F_2-derived F_3 families of 15 plants (hereinafter referred to as F_3) together with the parents were grown in a randomized block design with two replications during the two consecutive growing season 2014–2015 and 2015–2016 at CREA-CI (41°27′40.2″ N 15°30′04.5″ E). F_2 and F_3 seeds were individually hand-planted in single rows, 2 m length, and 0.5 m between rows.

The RIL population comprising 178 lines and the two parents were planted during the two consecutive growing seasons 2017–2018 and 2018–2019 (hereinafter referred to as F_6 and F_7, respectively) at the same experimental site. To simulate a standard open field sowing, a standard sowing density corresponding to approximately 350 seeds per square meter was carried out in single rows, 2 m long and 0.20 spaced, in a randomized block design with two replications. Whole plants of the F_2, F_3, and the two RIL generations (F_6 and F_7) were manually harvested at the end of June 2015, 2016, 2018 and 2019, respectively. Crop management was performed using standard cultivation methods. Growing season precipitation and temperature data were collected from the meteorological station of the CREA-CI.

2.2. Phenotypic Evaluation

Traits were measured both on a row and individual plant basis as follows: Heading date (HD) was recorded as days from the 1st of April in all growing seasons when 50% of the plants in a row were at GS59 [49]. Plant height (PH, cm) of individual F_2 and F_3 plants and ten randomly selected plants from RILs were measured at maturity. The juvenile growth habit trait (GH) was estimated by measuring the tiller angle between the last developed tillers and the ground level with a protractor at the maximum tillering stage (GS25 to GS29) by following UPOV [44] guidelines: 1, erect; 3, semi-erect; 5, intermediate; 7, semi-prostrate; and 9, prostrate. Tillering was monitored throughout the study period. Ten plants randomly selected on each single row were marked to facilitate identification at harvest. This was necessary for the F_6 and F_7 RIL generation with dense planting. At maturity, the number of tillers bearing spikes for each plant was counted, together with the number of fertile spikes. The tillering data were used to calculate the maximum number of tillers (TTN) and the number of fertile tillers (FTN). All phenotypic data were processed in the original form without any transformation. Principal component analysis (PCA) was performed using the mean values of all phenotypic data with the function

"prcomp" implemented in the *factoextra* v. 1.0.7 library under R environment v. 4.0.2. Pearson correlation coefficients (r) were calculated among traits using the "cor" function and the correlogram was constructed and visualized using the *Corrplot* package v. 0.84 implemented in R v. 4.0.2 [50]. Coefficient of variation was calculated as follows:

$$CV = Std/M \times 100 \tag{1}$$

where "Std" represents the standard deviation and "M" represents the mean for a trait. Broad-sense heritability (H^2) was estimated as follows:

$$H^2 = \sigma g/[\sigma g + (\sigma gy/y) + (\sigma e/\tau y)] \tag{2}$$

where σg is genotypic component of variance, σgy is the variance explained by interaction between genotypes and year, σe is the variance of residual effects, τ is the number of the repetitions, and y is the number of the year.

The Shapiro–Wilk (w) statistics was used to test the null hypothesis that the phenotypic data were normally distributed [51].

2.3. Linkage Maps Construction

Plant materials from F_2, F_6 generations, and both parents were genotyped with the wheat Illumina 25K Infinium single nucleotide polymorphism (SNP) array that was developed at the Trait Genetics (available online: http://www.traitgenetics.com, accessed on 24 June 2020). Both datasets were filtered by removing missing data (call rate > 10%) and rare alleles (MAF < 1%). Markers showing significant ($p < 0.01$) segregation distortion were also discarded.

The two filtered datasets were used to construct the genetic maps (hereinafter referred to as F_2 and RIL map) using the package *ASMap* v. 0.4.1 [52]. Linkage groups were constructed using the MSTmap algorithm [53] based on the *p*-value threshold set to 1×10^{-10} and 1×10^{-12} for F_2 and RIL populations, respectively. The Kosambi function was used to calculate the distance between markers and convert the recombination frequency into map distance (cM). The recombination fraction between all pairs of markers was estimated by the "est.rf" function to verify if each marker was placed in the right chromosome and in the correct order as compared with the Wen's reference map [54]. According to the Wen's reference map, some chromosomes were flipped through the "flip.order" function, whereas different linkage groups belonging to the same chromosome were merged using "mergeCross" function. The colinearity between the F_2 and F_6 linkage maps was evaluated by the Spearman rank correlation coefficient calculated by the R function "cor.test". A comparison between the obtained maps was performed by the R package *SOFIA* v. 1.0 [55].

2.4. QTL Mapping Approaches

The QTLs were detected for each trait in both generations by performing genome-wide composite interval mapping (gCIM), using the R software *QTL.gCIMapping.GUI* v.2.0 [56]. The first step was the binning of the redundant markers, as these markers have the same segregation in the population and bring no additional information to QTL analysis. The selected model was fixed and a walk speed for genome-wide scanning set to 1 cM. The LOD score threshold was set to 3.0 for both F_2:F_3 and RILs. A maximum likelihood (ML) function was used, the random seeds were set to 11,001, and the completing CIM in one neighborhood was set to "FALSE" for the F_2:F_3 population only. Moreover, the effects of QTLs, which include additive and dominance effects, were estimated by empirical Bayesian methods. The QTLs were named based on the recommended rules for gene symbolization in wheat (available online at https://wheat.pw.usda.gov/ggpages/wgc/98/Intro.htm, accessed on 15 January 2021).

2.5. Identification of Putative Candidate Genes

Putative candidate genes were identified within the QTL confidence intervals based on the annotation of the Chinese Spring genome, according to the IWGSC RefSeq v1.0 [57] (https://wheat-urgi.versailles.inra.fr/Seq-Repository/Annotation, accessed on 1 February 2021). The acronym of genes was assigned using the UNIPROT database (https://www.uniprot.org/, accessed on 1 February 2021). The sequence of the *PINE1* (LOC_Os12g42250) gene isolated in rice was retrieved by Gómez-Ariza et al. [58], whereas *PIF4* (LOC_Os12g41650) sequence was searched on the rice genome database available at https://shigen.nig.ac.jp/rice/oryzabase/ (accessed on 10 February 2021). The rice nucleotide sequences were used for a TBLASTN search against the genomes of the durum cultivar Svevo (http://www.gramene.org/, accessed on 10 February 2021). Then, the physical map position of the best sequence hits was compared to that of the genes identified in the QTL intervals, to investigate the correspondence.

Finally, all genes found in the QTL intervals were associated with a metabolic pathway by trait using the software MAPMAN [59].

3. Results

3.1. Phenotypic Evaluation and Correlation Analysis between Early and Late Generations

Mean values, ranges, coefficient of variation (CV), and broad-sense heritability (H^2) of the investigated traits were calculated for each of the four generations (Table 1). Significant differences between the mean values of the parents were observed in all generations for HD, GH, TTN, and FTN, except for PH in the late generations.

Table 1. Minimum, maximum, mean, standard deviations (St. Dev), coefficient of variation (CV), and heritability (H^2) for five traits in the F_2, F_3, F_6, and F_7 populations. Phenotipic values of both parents (Lankaodali, L and Rebelde, R) are also shown.

Trait	Acronym	Unit	L	R	Min	Max	Mean	St. Dev	CV%	H^2
Heading Date	HD	Day								
F_2			16.0	28.0	17.0	30.0	24.36	2.91	11.93	
F_3			23.0	30.0	22.0	33.0	27.07	2.74	10.13	0.74
F_6			19.5	25.0	17.0	34.0	23.88	3.50	14.64	
F_7			13.5	24.0	8.0	30.0	19.98	4.90	24.50	0.69
Juvenile Growth Habit	GH	Scale								
F_2			1.0	6.0	1.0	7.0	2.69	1.93	71.94	
F_3			2.0	5.0	1.0	9.0	5.70	1.77	31.10	0.30
F_6			2.5	5.0	1.4	9.0	5.45	1.42	26.11	
F_7			2.5	5.5	2.0	9.0	5.74	1.51	26.38	0.82
Plant Height	PH	cm								
F_2			49.0	75.0	35.0	110.0	66.14	12.68	19.18	
F_3			56.0	64.0	30.0	90.0	63.43	13.71	21.61	0.76
F_6			57.0	67.0	30.0	110.0	67.46	14.62	21.66	
F_7			54.5	60.5	30.0	100.0	67.67	13.32	19.68	0.83
Total Tiller Number	TTN	number								
F_2			17.0	42.0	10.0	56.0	30.25	10.17	33.61	
F_3			13.0	37.0	10.0	43.0	22.82	5.32	23.30	0.17
F_6			17.0	41.0	11.0	49.0	27.02	8.03	29.70	
F_7			12.0	29.4	8.33	41.0	22.94	6.52	28.44	0.37
Fertile tiller number	FTN	number								
F_2			15.0	36.0	7.0	54.0	28.10	9.81	34.90	
F_3			10.0	34.0	10.0	36.0	20.39	4.74	23.25	0.20
F_6			16.0	37.0	7.0	46.0	23.81	7.56	31.77	
F_7			9.6	16.2	3.0	37.5	18.23	6.92	37.93	0.46

The mean values of HD were higher in F_2 and F_3 than in F_6 and F_7, while the opposite was observed for PH. F_2 had the lowest mean value for GH, F_2 and F_6 showed the highest values in TTN and FTN. For the five traits, the CV ranged from 10.13 (HD) to 71.94% (GH) in the early generations and from 14.74 (HD) to 37.93% (FTN) in the late generations. The H^2 values ranged from 0.17 to 0.76 and from 0.37 to 0.83 in the early and in the late generations, respectively. The H^2 values higher than 0.69 were observed for HD and PH in early and RIL generations, while GH had H^2 higher in the RILs (0.82) than in the F_2/F_3 (0.30). The heritability of the TTN and FTN was low in both generations with the lowest value in the early generations (0.17 and 0.20 for TTN and FTN, respectively).

The Shapiro–Wilk test confirmed the normality of PH, TTN, and FTN data in F_2 and F_7 populations, with a right-skewed distribution for the last two traits. In addition, normality was also observed for the trait FTN in the F_3 and for the traits, GH and PH, in the F_6 generations. A bimodal distribution for HD was observed in early generations (F_2 and F_3) (Supplementary Figure S1).

The PCA analysis, based on the five morpho-physiological traits, showed a large variability within the four populations (Figure 1). The first two dimensions explained 70.1%, 69.9%, 66.5%, and 63.6% of the total variance in the F_2, F_3, F_6, and F_7 generations, respectively.
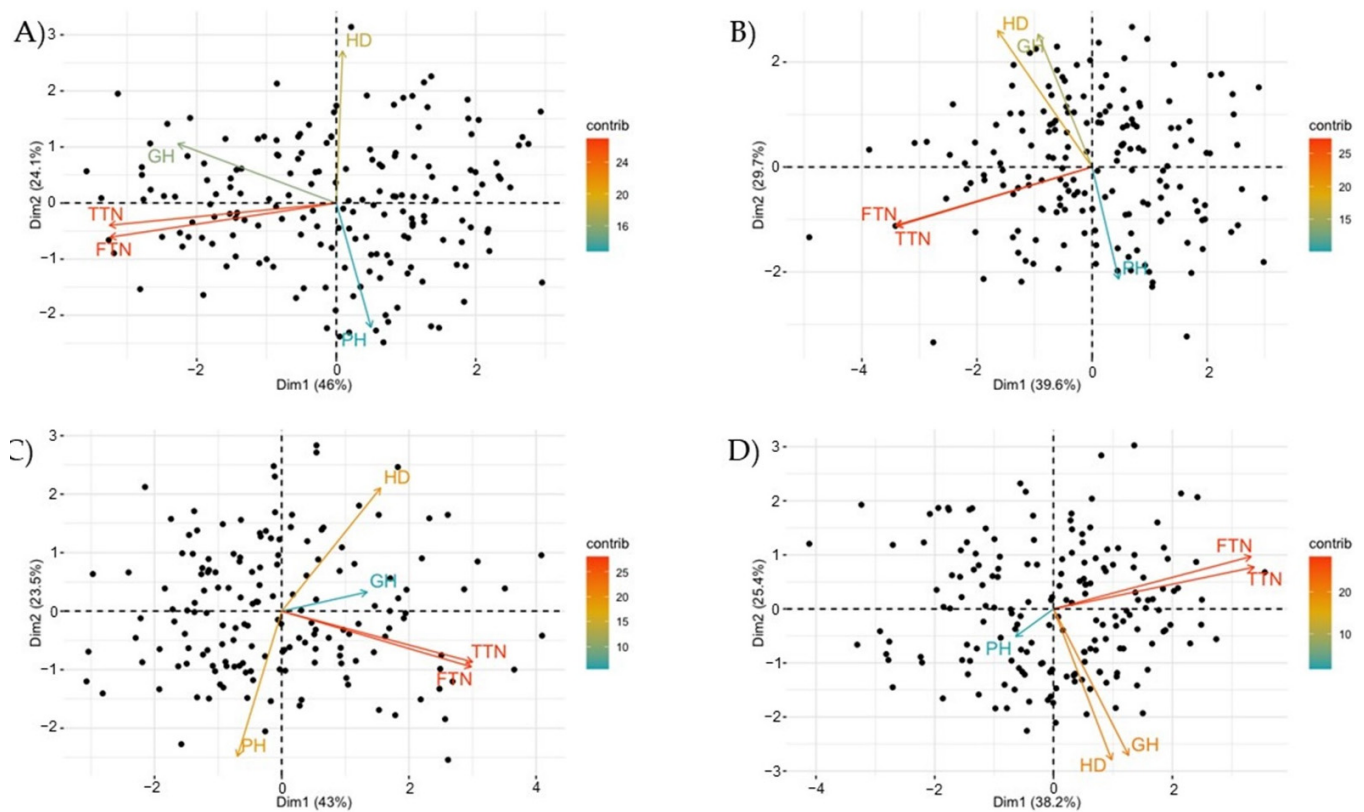
Figure 1. Principal component analysis (PCA) diagram showing the phenotypic variation and variable contribution in F_2 (**A**), F_3 (**B**), F_6 (**C**), and F_7 (**D**) generations. Black points correspond to genotypes, whereas the arrows represent the contribution of the variables to the total variation. HD, heading date; PH, plant height; GH, growth habit; TTN, total tiller number; FTN, fertile tiller number; contrib, contribution of variables to the principal axes expressed as a percentage (%).

The first component discriminated PH from the other traits in all populations, except for the HD in F_2. The second dimension discriminated HD and GH from PH, FTN, and TTN in all generations except for F_7.

Finally, Supplementary Figure S2 and Table S2 show that in the four generations, a significant positive correlation was observed between TTN and FTN (r > 0.82 and *p*-value < 1.33×10^{-44}), between GH and HD in F_3 (r = 0.40, *p*-value = 2.79×10^{-8}) and F_7 (r = 0.33, *p*-value = 7.55×10^{-6}), and between GH and TTN/FTN in F_2 (r = 0.45, *p*-value = 4.32×10^{-10} and r = 0.45, *p*-value = 4.66×10^{-10}), F_6 (r = 0.19, *p*-value = 1.40×10^{-2} and r = 0.21, *p*-value = 9.16×10^{-3}), and F_7 (r = 0.15, *p*-value = 5.13×10^{-2} and r = 0.11, *p*-value = 0.15). By contrast, a significant negative correlation was observed between PH and HD in F_3 (r = −0.28, *p*-value = 2.13×10^{-3}) and F_6 (r = −0.27, *p*-value = 7.55×10^{-6}).

3.2. Construction of F_2 and F_6 Linkage Maps and Their Colinearity

After filtering, 3684 and 3958 SNP variants were retained for F_2 and F_6, respectively, and used to build the two genetic maps. Thirty-nine and thirty-eight linkage groups were identified in F_2 and F_6 populations, respectively. The smaller linkage groups were joined to form the twenty-one chromosomes of *T. aestivum* L., based on the information available in the consensus map of Wen et al. [54]. The two genetic maps spanned 2486.97 and 3732.84 cM in length, for the F_2 and RILs, respectively, with an average marker density of 1.37 and 1 marker/cM (Supplementary Table S3).

The coverage was 47.49%, 36.82% and 15.69% for genome A, B, and D, respectively, in the F_2, and 46.58%, 42.28%, and 11.14% in the F_6.

The chromosomes length ranged from 5.01 (chr. 3D) to 231.56 cM (chr. 1B) with an average length of 118.43 cM in the F_2 map (Supplementary Table S4). Among the RILs, the chromosomes length varied between 3.93 (chr. 4D) and 360.26 cM (chr. 5B), with an average of 177.75 cM. The distance between adjacent markers for each chromosome ranged between 0.26 (chr. 3D) and 5.50 cM (chr. 7D) with an average distance of 1.15 cM in the F_2 map, and between 0.55 (chr. 2A) and 7.96 cM (chr. 7D) in the F_6, with an average of 1.50 marker/cM. The collinearity was calculated between the two genetic maps (Figure 2 and Supplementary Table S4). The Spearman rank correlation coefficient of each chromosome was calculated for the F_2 and F_6 linkage maps, ranging from −1 (chr. 7D) to 0.95 (chr. 1A) (Supplementary Table S4). Among all the twenty Spearman rank correlation coefficients, six were higher than 0.90 (chr. 1A, 2A, 3A, 5B, 6B, and 7A), and seven were comprised between 0.80 and 0.89 (1B, 2B, 4B, 5A, 6A, 6D, and 7B). Three chromosomes on D genome (2, 4, and 7) showed a negative correlation.
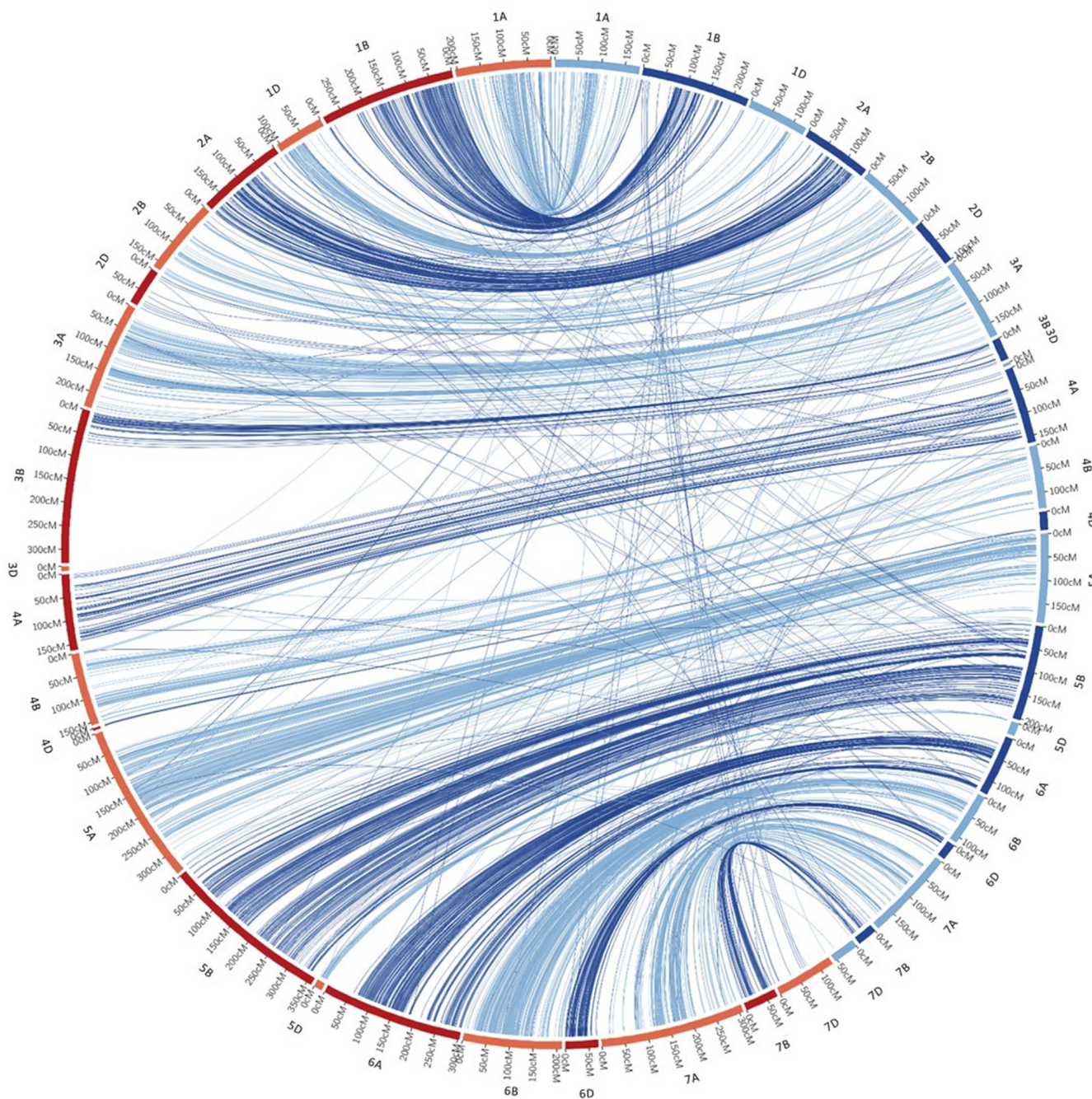
Figure 2. Circle plot showing the collinearity between the 21 linkage groups generated by F_2 (blue lines, right side) and F_6 (red lines, left side) populations.

3.3. QTL Identification for Different Traits

A total of 37 QTLs associated with the five morpho-physiological traits were detected using all datasets separately (F_2, F_3, F_6, and F_7), of which 28 and 10 were detected in the early (F_2 and F_3) and late (F_6–F_7) generations, respectively (Table 2). One QTL (*QGh-2D.1*) was identified both in F_3 and F_7, whereas three QTLs were identified in overlapped regions between F_2/F_3 and F_6/F_7 (Figure 3). The QTLs were distributed across all chromosomes except for 1D, 5D, 6A, 6B, 6D, and 7B. Twelve, sixteen and nine QTLs were mapped to the A, B, and D genomes, respectively. The phenotypic variation explained by an individual QTL was estimated between 0.53 (*QTtn-1A.1*) and 30.98% (*QHd-5A*). The LOD values ranged from 3.04 (*QFtn-4B*) to 18.78 (*QHd-5A*).

Table 2. QTLs significantly associated with the five morpho-physiological traits in the mapping populations. HD, heading date; PH, plant height; GH, juvenile growth habit; TTN, total tiller number; FTN, fertile tiller number; pop, population; chr., chromosome.

Trait	QTL	Chr.	Flanking Marker	Position (cM)	Pop	LOD [a]	R^2 (%) [b]	Add [c]	Dom [d]	Gene	Gene Reference [e]
HD	*QHd-2B.1*	2B	TG0015-IWB43273	42.72–44.25	F$_2$	5.60	3.82	0.80	0.00	*Ppd-B1*	[61]
										LEA	TraesCS2B01G158600
	QHd-2B.2	2B	AX-95186189-IWB55936	28.37–50.93	F$_7$	5.10	9.92	−1.44	-	*Ppd-B1*	[61]
										NAC	TraesCS2B01G075900
										RUBISCO	TraesCS2B01G079100
	QHd-2D	2D	IWB3771-IWB7001	9.17–24.99	F$_2$	4.59	4.09	−0.83	0.00	*Ppd-D1*	[62]
										Rht-8	[63]
										RUBISCO	TraesCS2D01G065100
										GA2OX2	TraesCS2D01G049700
										SLC	TraesCS2D01G055700
	QHd-4D	4D	IWB61486-IWB30224	13.86–25.95	F$_3$	3.63	6.10	−1.19	0.00	*Rht-D1*	[61]
	QHd-4D	4D	IWB61486-IWB30224	13.86–25.95	F$_2$	3.39	1.82	−0.55	0.00	*AP2/ERF*	TraesCS4D01G131200
										SLC	TraesCS4D01G127800
										ANT	TraesCS4D01G131200
										CO	TraesCS4D01G046200
										PIN	TraesCS4D01G125300
	QHd-5A	5A	IWA6961-AX-94636029	265.91–273.26	F$_6$	5.53	13.17	−1.00	-	*Vrn-A1*	TraesCS5A01G391700
	QHd-5A	5A	IWA6961-AX-94636029	265.91–273.26	F$_7$	18.78	30.98	−2.54	-	*AP2/ERF*	TraesCS5A01G398500
										GASA1	TraesCS5A01G405400
	QHd-7D	7D	IWA2545-AX-94418300	38.27–51.76	F$_6$	3.07	6.48	−0.70	-	*AGL*	TraesCS7D01G107000
	QHd-7D	7D	IWA2545-AX-94418300	38.27–51.76	F$_7$	12.55	16.68	−1.87	-	*ERF*	TraesCS7D01G107400
										SAUR	TraesCS7D01G160000
										AMY2	TraesCS7D01G160200
										ARF	TraesCS7D01G161900
										GRF	TraesCS7D01G166400
GH	*QGh-1B.1*	1B	IWB60063-IWB9661	126.01–128.22	F$_6$	6.42	12.37	0.43	-	*CO*	TraesCS1B01G300300
										ZC3H	TraesCS1B01G302100
	QGh-1B.2	1B	AX-94639048-IWB2222	117.28–118.88	F$_7$	5.70	9.31	0.42	-	*GID1a*	TraesCS1B01G265900
										Os20ox2	TraesCS1B02G274200
	QGh-2D.1	2D	IWB38687-IWB53594	94.78–100.55	F$_3$	3.31	3.65	0.49	0.00	*SLC*	TraesCS2D01G055700
	QGh-2D.1	2D	IWB38687-IWB53594	75.17–82.24	F$_6$	4.29	6.24	0.30	-	*RAA1*	TraesCS2D01G113700
										ZC3H	TraesCS2D01G115400
										CO	TraesCS2D01G121400
	QGh-2D.2	2D	IWB37711-IWB32004	10.76–17.87	F$_6$	3.33	8.48	−0.36	-	*Ppd-D1*	[61]
										NAC	TraesCS2D01G061500
										NPF2.2	TraesCS2D01G044000
										RAA1	TraesCS2D01G046600
										GA2OX2	TraesCS2D01G049700
										SWEET	TraesCS4B01G339600
	QGh-4B	4B	IWA7566-IWB12188	80.00–83.07	F$_3$	5.35	3.33	0.00	−0.67	*PINE1*	TraesCS4B01G342300
										SD1	TraesCS4B02G344800
										Os20ox	TraesCS4B02G344900
										SWEET	TraesCS4B01G339600
										CO	TraesCS4B01G340600
	QGh-5A	5A	IWA6961-AX-94636029	265.91–273.26	F$_6$	7.23	13.10	−0.44	-	*Vrn-A1*	TraesCS5A01G391700
	QGh-5A	5A	IWA6961-AX-94636029	265.91–273.26	F$_7$	10.21	22.60	−0.66	-	*NPF1.2*	TraesCS5A01G388000
										TRN1	TraesCS5A01G390900
										GASA1	TraesCS5A01G398500
										AP2/ERF	TraesCS5A01G405400
PH	*QPh-2D*	2D	IWB3771-IWB7001	9.17–24.99	F$_2$	3.06	2.28	2.91	0.00	*Ppd-D1,*	[62]
										Rht-8	[63]
										SWEET	TraesCS2D01G052100
										SCL	TraesCS2D01G055700
										RUBISCO	TraesCS2D01G065100
	QPh-4B.1	4B	IWB30623-IWB331	47.88–48.45	F$_2$	14.17	16.39	−7.80	0.00	*Rht-B1b*	[64]
										GAI	TraesCS4B01G043100
										CO	TraesCS4B01G045700
	QPh-4B.2	4B	AX-94545917-IWB25207	55.96–75.56	F$_6$	8.65	26.41	7.02	-	*LEA*	TraesCS4B01G327400
	QPh-4B.2	4B	AX-94545917-IWB25207	55.96–75.56	F$_7$	5.81	21.00	6.39	-	*AMY2*	TraesCS4B01G328000
										NAC	TraesCS4B01G328900

Table 2. *Cont.*

Trait	QTL	Chr.	Flanking Marker	Position (cM)	Pop	LOD [a]	R² (%) [b]	Add [c]	Dom [d]	Gene	Gene Reference [e]
	QPh-4D	4D	IWB12054-IWB61486	7.80–13.86	F₂	17.53	30.32	10.61	0.00	Rht-D1	[65]
	QPh-4D	4D	IWB12054-IWB61486	7.80–13.86	F₃	9.92	20.65	9.33	0.00	Rht-D1	[65]
										ZC3H	TraesCS4D01G000900
										ERF	TraesCS4D01G001200
										CO	TraesCS4D01G046200
										SLC	TraesCS4D01G054000
	QPh-5A	5A	IWB48095-IWB2075	149.90–150.76	F₃	3.45	1.79	0.00	−3.89	TEM1	[57]
										CLV3	TraesCS5A01G495600
TTN	QTtn-1A.1	1A	IWA6644-IWA6644	1.14–1.14	F₂	3.29	0.53	0.00	1.52	Gli-A1	TraesCS1A01G007200
										Glu-A3	TraesCS1A01G008000
	QTtn-1A.2	1A	IWA6553-IWA6553	90.06–90.06	F₂	11.77	2.42	0.00	3.24	n.a.	n.a.
	QTtn-1B.1	1B	IWA6294-IWA6294	137.25–137.25	F₂	10.60	4.22	3.03	0.00	LEA	TraesCS1B01G381200
	QTtn-2B.1	2B	IWA571-IWA571	122.08–122.08	F₂	7.06	1.48	0.00	−2.53	GA3OX2	TraesCS2B01G570800
										LEA	TraesCS2B01G571900
										ERF	TraesCS2B01G572500
	QTtn-2B.2	2B	IWB36228-IWB36228	138.76–138.76	F₂	4.29	1.47	1.78	0.00	SWEET	TraesCS2B01G593500
										YUCCA	TraesCS2B01G595700
	QTtn-3A	3A	IWB72078-IWB72078	44.14–44.14	F₂	17.91	4.06	0.00	4.20	TPS6	TraesCS3A01G289300
										PTST	TraesCS3A01G289800
	QTtn-3D	3D	IWB42792-IWB42792	5.01–5.01	F₂	3.57	1.24	1.64	0.00	LEA	TraesCS3D01G525900
										ERF	TraesCS3D01G521500
	QTtn-4A	4A	IWB60703-IWB60703	62.63–62.63	F₂	7.22	2.67	2.41	0.00	SUT	TraesCS4A01G334500
	QTtn-4B.1	4B	IWB6048-IWA7566	74.12–80.00	F₂	12.46	2.53	0.00	−3.32	LEA	TraesCS4B01G327400
										AMY2	TraesCS4B01G328000
										NAC	TraesCS4B01G328900
	QTtn-4B.2	4B	AX-94545917-IWB25207	55.96–75.56	F₆	3.74	10.49	−1.84	-	LEA	TraesCS4B01G327400
										AMY2	TraesCS4B01G328000
										NAC	TraesCS4B01G328900
	QTtn-4D	4D	IWB61486-IWB30224	13.86–25.95	F₂	5.05	1.03	0.00	2.12	Rht-D1	[65]
										AP2/ERF	TraesCS4D01G131200
										SLC	TraesCS4D01G127800
										ANT	TraesCS4D01G131200
										CO	TraesCS4D01G046200
										PIN	TraesCS4D01G125300
	QTtn-5A	5A	IWA3100-IWA3100	7.28–7.28	F₂	6.10	2.36	2.26	0.00	PIF4	TraesCS5A02G049600
	QTtn-5B	5B	IWB47364-IWB21455	157.44–158.92	F₂	3.84	0.61	0.00	−1.63	YUCCA	TraesCS5B01G530900
										LEA	TraesCS5B01G531400
	QTtn-7A.1	7A	IWB10707-IWB38357	0.28–15.90	F₂	6.92	1.52	0.00	2.57	NPF4.4	TraesCS7A01G073000
										YUCCA	TraesCS7A01G075400
										NR	TraesCS7A01G078500
										ERF	TraesCS7A01G128800
										SAUR	TraesCS7A01G129000
										CO	TraesCS7A01G132100
	QTtn-7A.2	7A	IWA6802-IWA3719	48.30–59.76	F₂	10.07	2.31	0.00	3.17	SuS1	TraesCS7A01G158900
										SAUR	TraesCS7A01G159100
										SWEET	TraesCS7A01G159800
										ARF	TraesCS7A01G160800
										GRF	TraesCS7A01G163400
										FRL1	TraesCS7A01G165600
	QTtn-7A.3	7A	IWA179-IWA7005	176.19–192.55	F₂	4.81	1.93	−2.05	0.00	YUCCA	TraesCS7A01G551000
										AGL	TraesCS7A01G552000
	QTtn-7B	7B	IWA2568-IWA4092	7.50–12.06	F₂	5.12	1.05	0.00	−2.13	LEA	TraesCS7B01G022400
										NPF5.5	TraesCS7B01G040100
FTN	QFtn-1B	1B	IWA6294-IWA6294	137.25–137.25	F₂	3.78	2.67	2.32	0.00	LEA	TraesCS1B01G381200
	QFtn-4B	4B	IWB7078-IWB30623	38.80–47.88	F₂	3.04	2.67	2.32	0.00	LEA	TraesCS4B01G035600
	QFtn-7A	7A	IWA6802-IWA3719	48.30–59.76	F₃	6.25	4.10	0.00	4.06	SuS1	TraesCS7A01G158900
										SAUR	TraesCS7A01G159100
										SWEET	TraesCS7A01G159800
										ARF	TraesCS7A01G160800
										GRF	TraesCS7A01G163400
										FRL1	TraesCS7A01G165600

[a] LOD, logarithm of the odds; [b] R², phenotypic variance explained (%) for each QTL; [c] Add, estimation of the proportion of genetic variance due to additive effects; [d] Dom, estimation of the proportion of genetic variance due to dominance effects; [e] Transcript ID refers to the Chinese Spring genome, according to the IWGSC RefSeq v1.0 [57], (https://wheat-urgi.versailles.inra.fr/Seq-Repository/Annotation, accessed on 10 February 2021).
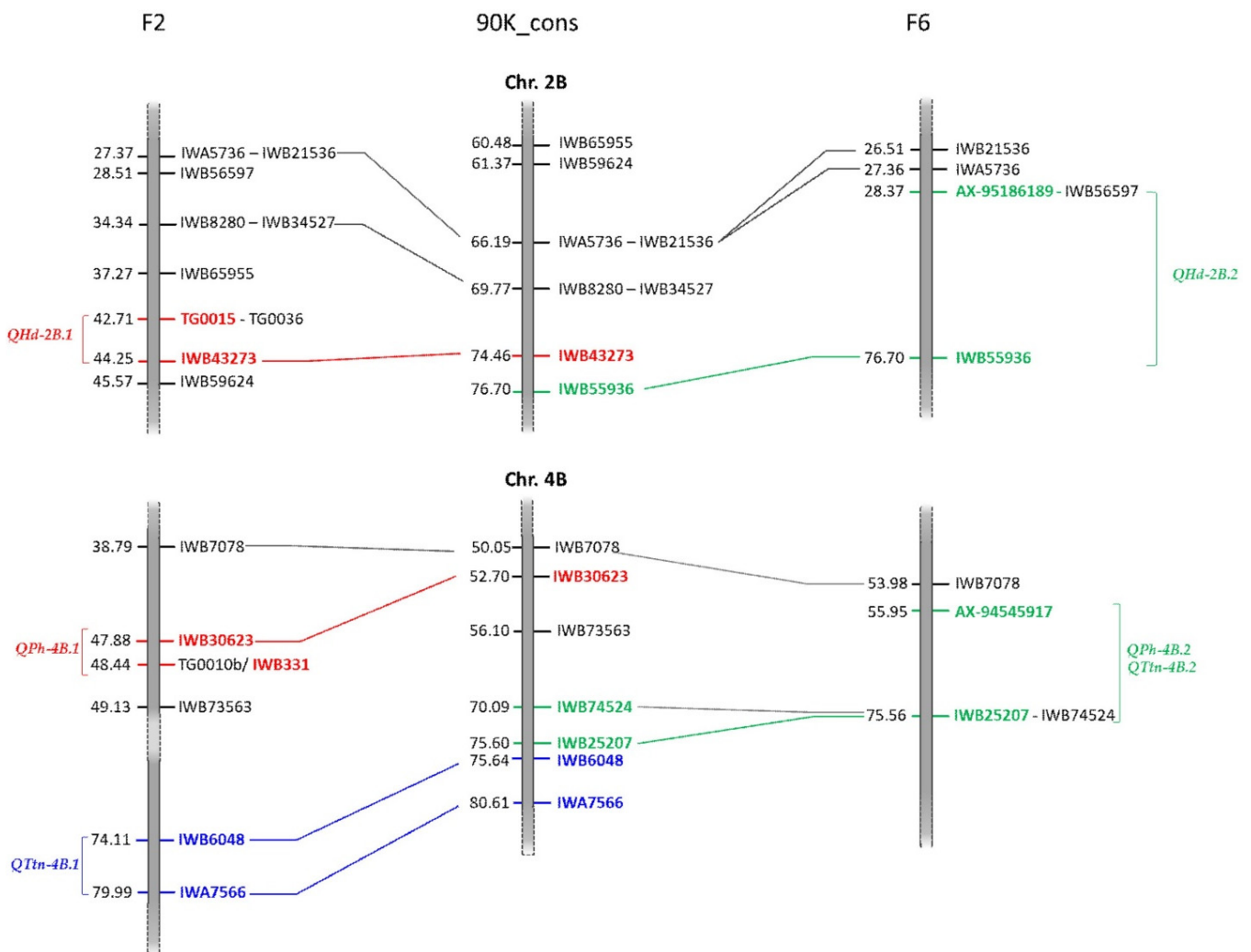
Figure 3. A graphical representation of the 2B and 4B linkage groups derived from the F_2 and F_6 maps and their comparison with the 90K consensus map. The distance between markers is in centimorgans (cM). The markers flanking the QTLs are colored in red (*QHd-2B.1* and *QPh-4B.1*) and blue (*QTtn-4B.1*) in F_2, while in green for the QTLs (*QHd-2B.2*, *QPh-4B.2*, and *QTtn-4B.2*) in F_6. Solid lines connect the genetic loci in common between the F_2 and F_6 genetic maps and the 90K consensus map [60].

For HD, six QTLs were identified on chromosomes 2B, 2D, 4D, 5A, and 7D, with individual QTL explaining 3.70–30.98% of the phenotypic variance. Of these, two QTLs were detected on chromosome 5A (*QHd-5A*) and 7D (*QHd-7D*), both in F_6 and F_7 populations, with individual QTLs explaining the highest phenotypic variance in the F_7 (R^2 = 30.98 and 16.68% for *QHd-5A* and *QHd-7D*, respectively). Two distinct QTLs (*QHd-2B.1* and *QHd-2B.2*) were found on chromosome 2B in the F_2 and RILs. However, the markers flanking the two QTLs were adjacent each other, with a distance of 2.24 cM according to the 90K consensus map [60] (Figure 3). One QTL (*QHd-4D*) was identified on chromosome 4D both in F_2 and F_3, exhibiting 1.82% and 6.10% of the phenotypic variance, respectively. One QTL (*QHd-2D*) was identified on chromosome 2D in F_2, with a negative additive effect.

Six QTLs were found for GH in both mapping populations (Table 2). Among all regions, a major QTL was found on chromosome 5A in late generations (F_6 and F_7), explaining the highest LOD scores and phenotypic variance (LOD = 7.23 and 10.21, R^2 = 13.1% and 22.6% in F_6 and F_7, respectively). On chromosome 1B, two adjacent regions were identified explaining a high fraction of phenotypic variance (12.37% and 9.31% for F_6 and F_7, respectively). Two QTLs were identified on chromosome 2D, of which, *QGh-2D.1* was

detected both in F$_3$ and F$_6$, while the *QGh-2D.2* was mapped only in F$_6$. Another QTL (*QGh-4B*) was found on chromosome 4B in F$_3$, with a dominance effect of −0.67.

A total of five QTLs were found associated with PH. Among all, the QTLs on chromosome 4B (*QPh-4B.1* and *QPh-4B.2*) explained a high proportion of phenotypic variation on F$_2$ (16.39%), F$_6$ (26.41%), and F$_7$ (21%). Although the markers flanking the *QPh-4B.1* and *QPh-4B.2* were different, the two regions could be considered overlapping, as showed in Figure 3. In fact, although many markers were not in common between the two genetic maps in this region, IWB7078 was the closest marker to *QPh-4B.1* and *QPh-4B.2.* On early generations, a significant QTL was mapped on chromosome 4D (*QPh-4D*). Another two QTLs (*QPh-2D* and *QPh-5A*) were identified, explaining 2.28 and 1.79% phenotypic variation, respectively.

The highest number of QTLs were detected for TTN. Seventeen QTLs were identified and distributed on almost all chromosomes (1A, 1B, 2B, 3A, 3D, 4A, 4B, 4D, 5A, 5B, 7A, and 7B). Among these, nine were identified by a single marker. All QTLs were detected in F$_2$ population, except for *QTtn-4B.2* (F$_6$), which showed the highest explained phenotypic variance (10.49%). The regions identified from the two QTLs, *QTtn-4B.1* and *QTtn-4B.2*, could be considered to be overlapping between F$_2$ and F$_6$ maps (Figure 3).

For FTN, three QTLs were found on the chromosomes 1B, 4B, and 7A in the early generations. Some QTLs showed a lower level of phenotypic variance ranging from 4.26% (*QFtn-7A*) to 2.67% (*QFtn-1B*).

Finally, we found that QTLs for different traits were located in the same chromosomal region. The flanking markers AX-94545917-IWB25207 identified a common region on chromosome 4B (*QPh-4B.2* and *QTtn-4B.2*) in late generations; the marker IWA6294 was associated with the *QTtn-1B.1* and *QFtn-1B* on chromosome 1B in F$_2$; the markers IWA6802-IWA3719 flanking the *QTtn-7A.2* and *QFtn-7A*; the *QHd-5A* and *QGh-5A* were delimited from the markers IWA6961-AX-94636029, while *QHd-2D* and *QPh-2D* from IWB3771-IWB7001 markers. The *QHd-4D* and *QTtn-4D* were flanking from IWB61486-IWB30224 markers.

3.4. Candidate Genes and Their Metabolic Pathway

Several genes modulating photoperiodic flowering pathway were annotated within QTLs (Table 2 and Supplementary File S1). Two transcriptor factors (TF) involved in flowering control, the *zinc-finger premature internode elongation 1* (*PINE1*, TraesCS4B01G342300) and the *phytocrome-interacting bHLH factor* (PIF4, TraesCS5A02G04960), were identified within QGh-4B and QTtn-5A, respectively. In addition, TFs that play a role in the regulation of flowering time and tillering, such as *DELLA protein gai* (*GAI*), *flowering-promoting factor* (*RAA1*), *Ap2-like ethylene-responsive* (*AP2/ERF*), *growth-regulating factor* (*GRF*), *ethylene-responsive* (*ERF*), *zinc finger protein constans* (*CO*), *Gras* (*SLC*), *AGAMOUS-MADS-box* (*AGL*), *zinc finger CCCH domain-containing* (*ZC3H*), and *NAC* domain were also annotated. We also identified genes that function in hormonal controlled steps of development, such as *gibberellin 2-beta-dioxygenase 2* (*GA2OX2*), *gibberel-lin 3-beta-dioxygenase 2* (*GA3OX2*), *gibberellin-regulated protein* (*GASA1*), *auxin response factor* (*ARF*), *auxin responsive SAUR* (*SAUR*), *flavin-containing monooxygenase* (*YUCCA*), *CLAVATA3/ESR* (*CLE*), and *tornado* (*TRN1*). The following genes, encoding sucrose and starch metabolisms and acting as a signal to control growth and differentiation, were identified: *trehalose-6-phosphate synthase 1* (*TPS6*), sugar transporters (*SWEET*), *sucrose synthase* (*SUS1*), *ribulose bisphosphate carboxylase* (*RUBISCO*), *alpha-amylase* (*AMY*), and *protein targeting to starch* (*PTST*). Finally, genes related to nitrogen metabolism, such as *nitrate reductase* (*NR*) and *nitrate transporter* (*NPF*), and seed storage (*γ-gliadin* and glutenin genes) were detected.

Supplementary Figure S3 summarizes the metabolic pathways in which the candidate genes are involved. Six different pathways were identified for HD, GH, PH, TTN, i.e., photosynthesis, secondary metabolism, tetrapyrrole, carbohydrate, lipid, and N-metabolism. The functional categories more represented for all traits were classified as fermentations and light reactions for photosynthesis, OPP, and the nitrogen assimilation (Supplementary Figure S3).

4. Discussion

Traits such as plant height, heading date, juvenile growth habit, and tiller number, historically, have been subjected to strong selective natural and artificial pressure, to improve the adaptation of bread wheat to different climatic conditions and to increase the grain yield [66–69]. However, these same traits are not only important for increasing crop yield potential, but they are also useful in determining the adaptation to climate change [7].

In the present work, the genetic control of five morpho-physiological traits was investigated, using two mapping populations derived from the same parents, to identify associated QTLs and candidate genes.

To achieve our aims, plants were deep phenotyped during four growing seasons. High heritability was recorded for PH and HD in both mapping populations. This was consistent with previous reports in wheat and also in other plant cereal species such as rice and barley, indicating a high response to selection of these traits [70–73]. By contrast, low heritability was found for GH, TTN, and FTN, as also recently reported by Marone et al. [44] and Bilgrami et al. [74] for juvenile growth habit and tiller number, respectively. Continuous distribution or absence of discrete segregating classes for PH, TTN, and FTN suggested that its inheritance is either determined by a large number of genes with small effects or by a few major genes with substantial environmental effects. The presence of transgressive segregants in all traits investigated suggested that each of the two parental cultivars had desirable and undesirable alleles in various proportions for loci governing these traits, as shown in Table 2.

More than 3000 high quality SNP markers were used to build the two genetic maps, and as expected, most of them were placed on genome A and B, in line with previous results [75–77]. Wen et al. [54] showed that the D genome had fewer markers than the A and B genomes in the high-density consensus map in common wheat.

The resulting maps were different in length, being 2486.97 cM in the F_2 and 3732.84 cM in the F_6. Similar to our results, Price and Tomos [78] obtained a map length of roughly 1280 cM in the F_2 population in rice, whereas a longer one (1680 cM) was observed in the F_6 produced by self-pollination of the same F_2 [79]. The observed differences were probably due to the different levels of heterozygosity, ranging about 50% and 5% in F_2 and F_6 RIL generations, respectively.

A total of 28 and 10 QTLs were found in the F_2/F_3 and RIL populations, respectively, for all traits (Table 2). Among all QTLs identified in the present study, only one was detected across both generations. However, the comparative QTL analysis of chromosomes 2B and 4B between F_2 and F_6 populations showed that three QTLs for HD, PH, and TTN could be considered to be adjacent and nearly overlapping. The results of the joint analysis indicate F_2/F_3 progenies have a higher power for detecting QTLs than the RIL populations. This is probably because the QTLs with dominant effects were only detected in the F_2:F_3 but not in the RIL generations. For quantitative traits with low heritability, such as TTN and FTN, the QTLs were identified only in early generations. This contrasted with what was expected, given that for quantitative traits, the precision of QTL mapping with an F_2 population may be relatively poor and, to solve this problem, a corresponding F_3 progeny was phenotyped, as proposed by Zhang and Xu [80]. However, in our study a possible explanation could be linked to the different sowing method adopted; spaced plantings in early generations allowed a better and more accurate evaluation of the tillering capacity of the wheat lines [81]. Furthermore, a higher marker density was observed in F_2 than in F_6, in the QTL regions. The low density of markers could affect the QTL analysis in the

RIL populations [12,82]. Indeed, Yi et al. [83], in a previous study, which included QTLs consistency across generations derived from the same cross, suggested that results largely depend on many factors including generations, environment, and genetic backgrounds.

Pearson rank between the assessed traits revealed that HD was correlated with the different morpho-physiological traits such as GH, PH, and TTN, in agreement with Bilgrami et al. [74], Rabbi and Hisam [77], and Mecha et al. [84]. In our study, several QTLs for different traits co-localized on the same chromosome, suggesting that they were not distributed evenly in the wheat genome, but they tended to cluster in particular chromosome regions (Table 2). According to their overlapping intervals, the regions on chromosome 5A, 2D, and 4D contained QTLs that were coincident for HD and GH, HD and PH, as well as HD and TTN, respectively. The two overlapping QTLs for TTN and FTN, found on chromosomes 1B and 7A, such as the common QTL for PH and TTN on chromosome 4B were expected. Other studies have confirmed that several QTLs/genes associated with canopy-architecture-related traits shared regions associated with yield-grain-related traits [85–88].

According to the physical map information obtained in this study and those of the major genes known in the literature to be responsible for the main morpho-phenolic wheat traits (i.e., *Vrn*, *Ppd*, and *Rht*), several co-localizations were found.

In particular, two overlapped QTLs for HD (*QHd-5A*) and GH (*QGh-5A*) contained the well-known gene *Vrn-A1* (TraesCS5A01G391700). Similarly, *QGh-2D.2* was found close to the photoperiod gene (*Ppd-D1*). This means that adaptation genes such as *Vrn* and *Ppd* influenced the expression of juvenile growth habit trait either because of linkage, or because they exert a pleiotropic effect on this trait, as previously suggested by Marone et al. [44]. As expected, we observed a co-localization among the QTLs *QHd-2B.1* and *QHd-2B.2* and the photoperiod gene *Ppd-B1* [89]. Similarly, the *QHd-2D* was only 4.5 Mb away from the *Ppd-D1* (*TraesCS2D02G079600*) gene. In addition, *QHd-4D* was found to be 7.2 Mb from the *Rht-D1* gene (*TraesCS4D02G040400*), suggesting that genes controlling plant height might also affect flowering time. In general, all the QTLs identified for HD had been extensively reported by the literature [38,61,90–92], confirming the strength of the use of two mapping populations in our work.

Similar results were also shown for the PH trait, which is one of the most studied [65]. Two QTLs (*QPh-4B.1* and *QPh-4B.2*) included the well-known dwarfing *Rht-B1* gene (TraesCS4B02G043100) and the region overlapped also with the one recently identified for plant height by Wang et al. [64], and with another QTL associated with maturity date [90]. In addition, the *Rht-D1* gene on chromosome 4D co-localized with the region identified by the *QPh-4D* in both early generations, sharing the common SNP marker RAC875_rep_c105718_304 with Zanke et al. [65].

Regarding TTN, all QTLs were identified in the early generations (with the exception of *QTtn-4B.2* in F_6) and distributed on almost all chromosomes (Table 2), confirming previous studies conducted in different genetic backgrounds and agronomic contexts [74,93]. *QTtn-4D* was detected very close to *Rht-D1* [65], similar to *QHd-4D*. The QFtn-4B detected on chromosome 4B was also interesting since it covered a genomic region close (6 Mb) to the *Rht-B1* gene. In the past, *Rht-B1b* and *Rht-D1b* were associated with increased productive tillers, which also contributed to increased yield [94–96]. Indeed, in our study we found the QTL for TTN in the same regions where the QTL for grain yield (*QTtn-1A.2*) and NDVI at tillering (*QTtn-7B*) were identified [97,98]. In this study a significant association between *Rht* genes and tillering traits was confirmed. The *QTtn-1A.1* identified by the SNP marker IWA6644 has been confirmed by a previous work by Bilgrami et al. [74].

It was observed that favorable alleles for each QTL were contributed by both parents, which was indicated by the additive effect of the QTLs. In addition, QTLs for TTN and FTN in the F_2 population showed both additive and dominant effects, suggesting the importance of both modes of gene action in conditioning tiller number and the greater difficulty in selection in late generations.

In addition to well-known genes involved in flowering time regulation (*Vrn*, *Ppd*, and *Rht*), QTL mapping detected candidate genes implicated in plant architectural traits including the regulation of the GA pathway, perception of light, photosynthesis, transport of photosynthates, and source-sink relationship. The role of these genes has been widely dissected in species such as rice and *Arabidopsis*, while they are still little investigated in wheat.

Gibberellin is a hormone that plays a central role in plant growth, organ development, and stress responses. In general, the existence of a regulatory network coordinating flowering and GA-dependent growth is well known. In our work we discovered genes coding enzymes of gibberellin biosynthesis (*Ga3ox*, *GA20ox*) and its receptors (DELLA-interacting protein *GID1* and *SD1*) associated with GH and TTN [99,100]. A barley GA 20-oxidase gene (*Hv20ox2*) has been proposed as a candidate for *sdw1/denso*, likely ortholog to the rice *sd1/Os20ox2* gene [101–103]. In barley, plants possessing the semi-dwarfing *sdw1/denso* gene have been characterized by prostrate GH, confirming our results [101]. In addition, further analysis revealed that the barley *sdw/denso* gene, has a pleiotropic effect on several agronomic traits such as plant height, heading, and flowering time [104].

Many zinc finger transcription factors have been found on chromosomes (1B, 2D, 4B, 4D, and 7A) such as CCCH-domain zinc finger proteins, which are known to be involved in plant growth habit and in leaf angle regulation [105]. Our findings confirmed the role of these transcription factors in determining the bread wheat GH, as reported in durum wheat [44].

Among its various functions, GA promotes the phenomenon of stem and leaf elongation [99]. In the flowering plants, altering internode length permits plants to vertically shift the distribution of their leaves and buds attached at nodes, changing their growth habit. Benefits of internode elongation at flowering include inflorescence escape from soilborne pests, outcompeting neighbors, and potential for diversified pollination and wider seed dispersal. In our work, the gene *PINE1* was a strong candidate associated with GH. It was recently identified in rice as a transcription factor involved in coordinating internode elongation and photoperiodic signals. It regulates the reduction of the sensitivity of the stem to gibberellin, with a consequent promotion of flowering [58].

In addition, we found a TF belonging to the *NAC* family associated with all traits. The *NAC* genes coding for TF have been shown to influence plant height through regulating the key genes in the GA pathway, as well as flowering time [106]. It has been observed that the *OsNAC2* promotes shoot branching; indeed, its overexpression resulted in more tillers [107]. Transgenic plants that constitutively expressed *OsNAC2* had shorter internodes, shorter spikelets, and were more insensitive to gibberellic acid. In addition, the *ERF* genes that we identified in QTLs related to TTN, trigger the upregulation of the internode elongation, through an increase in bioactive GA levels [108].

Plants alter their morphology to avoid the risk shading, through changes associated with the light spectrum and intensity. The responses to shade avoidance include variation in the hypocotyl and stem and activation of multiple hormones such as auxin, ethylene, and GA. The transcription factor *PIF4*, which we found within QTLs for TTN, is activated by the photoreceptors signal via separate pathways in leaf responses in *A. thaliana*. *PIF4* is a target for GA signaling through interaction with DELLA proteins, but also *GA20ox* and *GA3ox* expression, with a mechanism regulation currently unknown. It has been demonstrated that by destabilizing DELLAs, GA signaling promotes *PIF4* function [99,109].

In addition, during the early growth phase and under abiotic stress conditions, *PIF4* promotes auxin biosynthesis genes such as *YUCCA*, enhancing tissue auxin level that regulates small auxin up-RNA (*SAUR*) genes responsible for hypocotyl elongation when grown under light conditions [110–112].

Another important gene is the sucrose-signaling metabolite synthase *trehalose 6-phosphate synthase* (*TPS6*) located in the interval of the *Q.Ttn-3A*, which showed the higher LOD (17.91). This gene encodes what is considered to be a potent signaling molecule in plants for embryogenesis and normal postembryonic growth and development. Wahl et al. [113] indicated that the *TPS6* gene is required for timely initiation of flowering. In *Arabidopsis*, Fichtner et al. [114] suggested that the *TPS6* gene has two different functions depending on some parts of the plant and some developmental stages, both as a signal and as a negative feedback regulator of sucrose levels.

Finally, we found genes involved in nitrogen metabolism and carbohydrate assimilation (*RUBISCO*) and metabolism (*SUS*) associated with all traits. In *Arabidopsis*, it has been demonstrated that there is a significant interaction among nitrate, carbohydrates, *RUBISCO,* and the starch accumulations that affect plant growth and development, stress responses, and signal molecules [111,115,116]. The selected genes underlying the QTL regions represent a partial selection of genes that could regulated the traits investigated, therefore, further studies are needed to validate the causative genes.

5. Conclusions

The results of the present study show that QTL mapping results obtained from populations derived from founding parents at different generations are reliable. The exploitation of the two mapping populations made it possible to identify all the main regions of the morphological characters and even identify new regions of interest especially for low heritability characters such as GH ant tiller number. The QTLs detected in early generation are more than those in late generation, especially for those minor QTLs. Further studies are needed to confirm the chromosomal regions responsible for low heritability traits such as TTN and FTN. For these traits, it will be necessary to utilize spaced plantings to properly assess tillering habits of wheat cultivars because plants grown at high population densities in grower production fields are not likely to represent full tillering potential of a line/genotype. It was particularly interesting to observe the strong interaction between the adaptation genes and the morpho-physiological characteristics of the plants. It is evident, in fact, that the genes, in the past, that were fundamental for increasing productivity, will also be so in the near future as they are also responsible for the characters indirectly associated with the new climate scenario. This requires an in-depth study of the effect of allelic variants of adaptation genes by exploiting modern genomic technologies.

Supplementary Materials: The following are available online at https://www.mdpi.com/article/10.3390/genes12040604/s1, Table S1: Shapiro–Wilk test results. Normality test on the trait distributions among the generations using the Shapiro–Wilk test, Table S2: Phenotypic correlations among the five investigated traits. r = Pearson correlation coefficients. HD, heading date; PH, plant height; GH, growth habit; TTN, total tiller number; FTN, fertile tiller number, Table S3: Genetic map features. Main map characteristics concerning genetics maps constructed on F_2 and F_6 generations, Table S4: Genetic map data summary. Distribution of SNP markers across the twenty-one chromosomes in the F_2 and F_6 genetic maps. Chromosome length (cM), distance (cM), number of markers in common between F_2 and F_6, and coefficient of collinearity (Rho) were reported, Figure S1: Phenotypic distribution for the five traits across the F_2 (grey bars), F_3 (orange bars), F_6 (red bars), and F_7 (green bars). The *x*-axis represents phenotypic values, whereas the *y*-axis corresponds to density. Phenotypic values of parental lines Lankaodali (L) and Rebelde (R) are also shown. HD, heading date; PH, plant height; GH, growth habit; TTN, total tiller number; FTN, fertile tiller number, Figure S2: Pearson's correlation matrix for the five traits measured across the F_2 (A), F_3 (B), F_6 (C), and F_7 (D) populations. The square blank refers to the Pearson's correlation test yielded a non-significant *p*-value ($p > 0.05$). HD, heading date; PH, plant height; GH, growth habit; TTN, total tiller number; FTN, fertile tiller number, Figure S3: MapMan analysis. The blue squares indicated the major pathways of metabolic processes in which candidate genes were involved. HD, heading date; PH, plant height; GH, growth habit; TTN, total tiller number; FTN, fertile tiller number, File S1: List of candidate genes within QTLs annotated using the Svevo durum wheat genomic sequence. HD, heading date; PH, plant height; GH, growth habit; TTN, total tiller number; FTN, fertile tiller number.

References

1. FAO. Early Outlook for 2021 Crops. 2021. Available online: http://www.fao.org/worldfoodsituation/csdb/en/ (accessed on 15 April 2021).
2. Ray, D.K.; Mueller, N.D.; West, P.C.; Foley, J.A. Yield Trends Are Insufficient to Double Global Crop Production by 2050. *PLoS ONE* **2013**, *8*, 6. [CrossRef]
3. Hunter, M.C.; Smith, R.G.; Schipanski, M.; Atwood, L.W.; Mortensen, D.A. Agriculture in 2050: Recalibrating targets for sustainable intensification. *Bioscience* **2017**, *67*, 386–391. [CrossRef]
4. Zhao, C.; Liu, B.; Piao, S.; Wang, X.; Lobell, D.B.; Huang, Y.; Huang, M.; Yao, Y.; Bassu, S.; Ciais, P.; et al. Temperature increase reduces global yields of major crops in four independent estimates. *Proc. Natl. Acad. Sci. USA* **2017**, *114*, 9326–9331. [CrossRef]
5. Barrett, B.; Bayram, M.; Kidwell, K.; Weber, W.E. Identifying AFLP and microsatellite markers for vernalization response gene Vrn-B1 in hexaploid wheat using reciprocal mapping populations. *Plant Breed* **2002**, *121*, 400–406. [CrossRef]
6. Reynolds, M.; Foulkes, M.J.; Slafer, G.A.; Berry, P.; Parry, M.A.; Snape, J.W.; Angus, W.J. Raising yield potential in wheat. *J. Exp. Bot.* **2009**, *60*, 1899–1918. [CrossRef] [PubMed]
7. De Vita, P.; Taranto, T. Durum wheat (*Triticum turgidum* ssp. *durum*) breeding to meet the challenge of climate change. In *Advances in Plant Breeding Strategies: Cereals*; Al-Khayri, J.M., Jain, S.M., Johnson, D.V., Eds.; Springer: Berlin/Heidelberg, Germany, 2019; pp. 471–524.
8. Peng, J.; Richards, D.E.; Hartley, N.M.; Murphy, G.P.; Devos, K.M.; Flintham, J.E.; Beales, J.; Fish, L.J.; Worland, A.J.; Pelica, F.; et al. Green revolution'genes encode mutant gibberellin response modulators. *Nature* **1999**, *400*, 256–261. [CrossRef] [PubMed]
9. Worland, A.J.; Korzun, V.; Röder, M.S.; Ganal, M.W.; Law, C.N. Genetic analysis of the dwarfing gene *Rht8* in wheat. Part II. The distribution and adaptive significance of allelic variants at the *Rht8* locus of wheat as revealed by microsatellite screening. *Theor. Appl. Genet.* **1998**, *96*, 1110–1120. [CrossRef]
10. Giunta, F.; De Vita, P.; Mastrangelo, A.M.; Sanna, G.; Motzo, R. Environmental and genetic variation for yield-related traits of durum wheat as affected by development. *Front. Plant Sci.* **2018**, *9*, 1–19. [CrossRef] [PubMed]
11. Donald, C.M. The breeding of crop ideotypes. *Euphytica* **1968**, *17*, 385–403. [CrossRef]
12. Taranto, F.; Nicolia, A.; Pavan, S.; De Vita, P.; D'Agostino, N. Biotechnological and digital revolution for climate-smart plant breeding. *Agronomy* **2018**, *8*, 277. [CrossRef]
13. Doerge, R.W. Mapping and analysis of quantitative trait loci in experimental populations. *Nat. Rev. Genet.* **2002**, *3*, 43–52. [CrossRef]
14. He, P.; Li, J.Z.; Zheng, X.W.; Shen, L.S.; Lu, C.F.; Chen, Y.; Zhu, L.H. DH and RIL Populations Derived from the Same Rice Cross. *Distribution* **2001**, *41*, 1240–1246.
15. Staub, J.E.; Serquen, F.C.; Gupta, M. Genetic markers, map construction, and their application in plant breeding. *HortScience* **1996**, *31*, 729–740. [CrossRef]
16. Ferreira, A.; da Silva, M.F.; da Costa e Silva, L.; Cruz, C.D. Estimating the effects of population size and type on the accuracy of genetic maps. *Genet. Mol. Biol.* **2006**, *29*, 187–192. [CrossRef]
17. Li, Z.; Peng, T.; Xie, Q.; Han, S.; Tian, J. Mapping of QTL for tiller number at different stages of growth in wheat using double haploid and immortalized F2 populations. *J. Genet.* **2010**, *89*, 409–415. [CrossRef] [PubMed]
18. Clark, A.J.; Sarti-Dvorjak, D.; Brown-Guedira, G.; Dong, Y.; Baik, B.K.; Van Sanford, D.A. Identifying rare FHB-resistant segregants in intransigent backcross and F2 winter wheat populations. *Front. Microbiol.* **2016**, *7*, 1–14. [CrossRef]
19. Gill, H.S.; Li, C.; Sidhu, J.S.; Liu, W.; Wilson, D.; Bai, G.; Gill, B.S.; Sehgal, S.K. Fine mapping of the wheat leaf rust resistance gene *Lr42*. *Int. J. Mol. Sci.* **2019**, *20*, 2445. [CrossRef]

20. Khlestkina, E.K.; Röder, M.S.; Börner, A. Mapping genes controlling anthocyanin pigmentation on the glume and pericarp in tetraploid wheat (*Triticum durum* L.). *Euphytica* **2010**, *171*, 65–69. [CrossRef]

21. Kumar, A.; Sandhu, N.; Venkateshwarlu, C.; Priyadarshi, R.; Yadav, S.; Majumder, R.R.; Singh, V.K. Development of introgression lines in high yielding, semi-dwarf genetic backgrounds to enable improvement of modern rice varieties for tolerance to multiple abiotic stresses free from undesirable linkage drag. *Sci. Rep.* **2020**, *10*, 1–13. [CrossRef]

22. Park, K.J.; Sa, K.J.; Koh, H.J.; Lee, J.K. QTL analysis for eating quality-related traits in an F2:3 population derived from waxy corn × sweet corn cross. *Breed. Sci.* **2013**, *63*, 325–332. [CrossRef]

23. Scheben, A.; Severn-Ellis, A.; Patel, D.; Pradhan, A.; Rae, S.; Batley, J.; Edwards, D. Linkage mapping and QTL analysis of flowering time using ddRAD sequencing with genotype error correction in *Brassica napus*. *BMC Plant Biol.* **2020**, *20*, 546. [CrossRef]

24. Branham, S.E.; Levi, A.; Wechter, W.P. QTL mapping identifies novel source of resistance to fusarium wilt race 1 in *Citrullus amarus*. *Plant Dis.* **2019**, *103*, 984–989. [CrossRef]

25. Yogendra, K.N.; Ramanjini Gowda, P.H. Phenotypic and molecular characterization of a tomato (*Solanum lycopersicum* L.) F2 population segregation for improving shelf life. *Genet. Mol. Res.* **2013**, *12*, 506–518. [CrossRef] [PubMed]

26. Li, L.; Zhao, S.; Su, J.; Fan, S.; Pang, C.; Wei, H.; Wang, H.; Gu, L.; Zhang, C.; Liu, G.; et al. High-density genetic linkage map construction by F2 populations and QTL analysis of early-maturity traits in upland cotton (*Gossypium hirsutum* L.). *PLoS ONE* **2017**, *12*, 1–17. [CrossRef] [PubMed]

27. Burr, B.; Burr, F.A.; Thompson, K.H.; Albertson, M.C.; Stuber, C.W. Gene mapping with recombinant inbreds in maize. *Genetics* **1988**, *118*, 519–526. [CrossRef]

28. Cowen, N.M. The use of replicated progenies in marker-based mapping of QTL's. *Theor. Appl. Genet.* **1988**, *75*, 857–862. [CrossRef]

29. Lander, E.S.; Botstein, D. Mapping mendelian factors underlying quantitative traits using RFLP linkage maps. *Genetics* **1989**, *121*, 185–199. [CrossRef] [PubMed]

30. Knapp, S.J.; Bridges, W.C. Using molecular markers to estimate quantitative trait locus parameters: Power and genetic variances for unreplicated and replicated progeny. *Genetics* **1990**, *126*, 769–777. [CrossRef]

31. Jansen, R.C. Quantitative trait loci in inbred lines. In *Handbook of Statistical Genetics*; John Wiley & Sons, Ltd.: Hoboken, NJ, USA, 2004.

32. Haley, C.S.; Andersson, L. Linkage mapping of quantitative trait loci in plants and animals. In *Genome Mapping: A Practical Approach*; Oxford University Press: Oxford, UK, 1997.

33. Börner, A.; Schumann, E.; Fürste, A.; Cöster, H.; Leithold, B.; Röder, M.S.; Weber, W.E. Mapping of quantitative trait loci determining agronomic important characters in hexaploid wheat (*Triticum aestivum* L.). *Theor. Appl. Genet.* **2002**, *105*, 921–936. [CrossRef]

34. Wang, R.X.; Hai, L.; Zhang, X.Y.; You, G.X.; Yan, C.S.; Xiao, S.H. QTL mapping for grain filling rate and yield-related traits in RILs of the Chinese winter wheat population Heshangmai x Yu8679. *Theor. Appl. Genet.* **2009**, *118*, 313–325. [CrossRef]

35. Wang, Z.; Wu, X.; Ren, Q.; Chang, X.; Li, R.; Jing, R. QTL mapping for developmental behavior of plant height in wheat (*Triticum aestivum* L.). *Euphytica* **2010**, *174*, 447–458. [CrossRef]

36. Lin, F.; Xue, S.L.; Tian, D.G.; Li, C.J.; Cao, Y.; Zhang, Z.Z.; Zhang, C.Q.; Ma, Z.Q. Mapping chromosomal regions affecting flowering time in a spring wheat RIL population. *Euphytica* **2008**, *164*, 769–777. [CrossRef]

37. Sourdille, P.; Snape, J.W.; Cadalen, T.; Charmet, G.; Nakata, N.; Bernard, S.; Bernard, M. Detection of QTL for heading time and photoperiod response in wheat using a doubled-haploid population. *Genome* **2000**, *43*, 487–494. [CrossRef]

38. Guedira, M.; Xiong, M.; Hao, Y.F.; Johnson, J.; Harrison, S.; Marshall, D.; Brown-Guedira, G. Heading date QTL in winter wheat (*Triticum aestivum* L.) coincide with major developmental genes VERNALIZATION1 and PHOTOPERIOD1. *PLoS ONE* **2016**, *11*, 1–21. [CrossRef]

39. Wang, Z.; Liu, Y.; Shi, H.; Mo, H.; Wu, F.; Lin, Y.; Gao, S.; Wang, J.; Wei, Y.; Liu, C.; et al. Identification and validation of novel low-tiller number QTL in common wheat. *Theor. Appl. Genet.* **2016**, *129*, 603–612. [CrossRef]

40. Naruoka, Y.; Talbert, L.E.; Lanning, S.P.; Blake, N.K.; Martin, J.M.; Sherman, J.D. Identification of quantitative trait loci for productive tiller number and its relationship to agronomic traits in spring wheat. *Theor. Appl. Genet.* **2011**, *123*, 1043–1053. [CrossRef]

41. Hu, Y.; Ren, T.; Li, Z.; Tang, Y.; Ren, Z.; Yan, B. Molecular mapping and genetic analysis of a QTL controlling spike formation rate and tiller number in wheat. *Gene* **2017**, *634*, 15–21. [CrossRef] [PubMed]

42. Ren, T.; Hu, Y.; Tang, Y.; Li, C.; Yan, B.; Ren, Z.; Tan, F.; Tang, Z.; Fu, S.; Li, Z. Utilization of a Wheat55K SNP array for mapping of major QTL for temporal expression of the tiller number. *Front. Plant Sci.* **2018**, *9*, 1–12. [CrossRef]

43. Liu, J.; Tang, H.; Qu, X.; Liu, H.; Li, C.; Tu, Y.; Li, S.; Habib, A.; Mu, Y.; Dai, S.; et al. A novel, major, and validated QTL for the effective tiller number located on chromosome arm 1BL in bread wheat. *Plant Mol. Biol.* **2020**, *104*, 173–185. [CrossRef] [PubMed]

44. Marone, D.; Rodriguez, M.; Saia, S.; Papa, R.; Rau, D.; Pecorella, I.; Laidò, G.; Pecchioni, N.; Lafferty, J.; Rapp, M.; et al. Genome-wide association mapping of prostrate/erect growth habit in winter durum wheat. *Int. J. Mol. Sci.* **2020**, *21*, 394. [CrossRef] [PubMed]

45. Cobb, J.N.; Biswas, P.S.; Platten, J.D. Back to the future: Revisiting MAS as a tool for modern plant breeding. *Theor. Appl. Genet.* **2019**, *132*, 647–667. [CrossRef]

46. Collard, B.C.Y.; Jahufer, M.Z.Z.; Brouwer, J.B.; Pang, E.C.K. An introduction to markers, quantitative trait loci (QTL) mapping and marker-assisted selection for crop improvement: The basic concepts. *Euphytica* **2005**, *142*, 169–196. [CrossRef]
47. Asíns, M.J. Present and future of quantitative trait locus analysis in plant breeding. *Plant Breed.* **2002**, *121*, 281–291. [CrossRef]
48. Su, Z.; Hao, C.; Wang, L.; Dong, Y.; Zhang, X. Identification and development of a functional marker of *TaGW2* associated with grain weight in bread wheat (*Triticum aestivum* L.). *Theor. Appl. Genet.* **2011**, *122*, 211–223. [CrossRef] [PubMed]
49. Zadoks, J.C.; Chang, T.T.; Konzak, C.F. A decimal code for the growth stages of cereals. *Weed Res.* **1974**, *14*, 415–421. [CrossRef]
50. Wei, T.; Simko, V.; Levy, M.; Xie, Y.; Jin, Y.; Zemla, J. Package 'corrplot'. *Statistician* **2017**, *56*, 24.
51. Royston, P. Approximating the Shapiro-Wilk W-test for non-normality. *Stat. Comput.* **1992**, *2*, 117–119. [CrossRef]
52. Taylor, J.; Butler, D. R package ASMap: Efficient genetic linkage map construction and diagnosis. *J. Stat. Softw.* **2017**, *79*, 1–29. [CrossRef]
53. Wu, Y.; Bhat, P.R.; Close, T.J.; Lonardi, S. Efficient and accurate construction of genetic linkage maps from the minimum spanning tree of a graph. *PLoS Genet.* **2008**, *4*, e1000212. [CrossRef]
54. Wen, W.; He, Z.; Gao, F.; Liu, J.; Jin, H.; Zhai, S.; Qu, Y.; Xia, X. A high-density consensus map of common wheat integrating four mapping populations scanned by the 90k SNP array. *Front. Plant Sci.* **2017**, *8*, 1–14. [CrossRef]
55. Diaz-Garcia, L.; Covarrubias-Pazaran, G.; Schlautman, B.; Zalapa, J. SOFIA: An R Package for enhancing genetic visualization with circos. *J. Hered.* **2017**, *108*, 443–448. [CrossRef]
56. Zhang, Y.W.; Wen, Y.J.; Dunwell, J.M.; Zhang, Y.M. QTL.gCIMapping.GUI v2.0: An R software for detecting small-effect and linked QTL for quantitative traits in bi-parental segregation populations. *Comput. Struct. Biotechnol. J.* **2020**, *18*, 59–65. [CrossRef]
57. Appels, R.; Eversole, K.; Feuillet, C.; Keller, B.; Rogers, J.; Stein, N.; Pozniak, C.J.; Choulet, F.; Distelfeld, A.; Poland, J.; et al. Shifting the limits in wheat research and breeding using a fully annotated reference genome. *Science* **2018**, *361*. [CrossRef]
58. Gómez-Ariza, J.; Brambilla, V.; Vicentini, G.; Landini, M.; Cerise, M.; Carrera, E.; Shrestha, R.; Chiazzotto, R.; Galbiati, F.; Caporali, E.; et al. A transcription factor coordinating internode elongation and photoperiodic signals in rice. *Nat. Plants* **2019**, *5*, 358–362. [CrossRef]
59. Thimm, O.; Bläsing, O.; Gibon, Y.; Nagel, A.; Meyer, S.; Krüger, P.; Selbig, J.; Müller, L.A.; Rhee, S.Y.; Stitt, M. MAPMAN: A user-driven tool to display genomics data sets onto diagrams of metabolic pathways and other biological processes. *Plant J.* **2004**, *37*, 914–939. [CrossRef]
60. Wang, S.; Wong, D.; Forrest, K.; Allen, A.; Chao, S.; Huang, B.E.; Maccaferri, M.; Salvi, S.; Milner, S.G.; Cattivelli, L.; et al. Characterization of polyploid wheat genomic diversity using a high-density 90 000 single nucleotide polymorphism array. *Plant Biotechnol. J.* **2014**, *12*, 787–796. [CrossRef]
61. Zanke, C.; Ling, J.; Plieske, J.; Kollers, S.; Ebmeyer, E.; Korzun, V.; Argillier, O.; Stiewe, G.; Hinze, M.; Beier, S.; et al. Genetic architecture of main effect QTL for heading date in European winter wheat. *Front. Plant Sci.* **2014**, *5*, 1–13. [CrossRef] [PubMed]
62. Available online: https://wheat.pw.usda.gov/cgi-bin/cmap/viewer?mapMenu=1&featureMenu=1&corrMenu=1&displayMenu=1&advancedMenu=1&ref_map_accs=Wheat_Yr_genes_and_QTL_2D&sub=Draw+Selected+Maps&ref_map_set_acc=Wheat,%20Yr%20genes%20and%20QTL%202D&data_source=GrainGenes&highlight=%22Ppd1%22&label_features=all (accessed on 15 April 2021).
63. Lozada, D.N.; Carter, A.H. Insights into the genetic architecture of phenotypic stability traits in winter wheat. *Agronomy* **2020**, *10*, 368. [CrossRef]
64. Wang, Z.; Hu, H.; Jiang, X.; Tao, Y.; Lin, Y.; Wu, F.; Hou, S.; Liu, S.; Li, C.; Chen, G.; et al. Identification and Validation of a Novel Major Quantitative Trait Locus for Plant Height in Common Wheat (*Triticum aestivum* L.). *Front. Genet.* **2020**, *11*, 1–10. [CrossRef]
65. Zanke, C.D.; Ling, J.; Plieske, J.; Kollers, S.; Ebmeyer, E.; Korzun, V.; Argillier, O.; Stiewe, G.; Hinze, M.; Neumann, K.; et al. Whole genome association mapping of plant height in winter wheat (*Triticum aestivum* L.). *PLoS ONE* **2014**, *9*, e113287. [CrossRef] [PubMed]
66. Richards, R.A. A tiller inhibitor gene in wheat and its effect on plant growth. *Aust. J. Agric. Res.* **1988**, *39*, 749–757. [CrossRef]
67. Law, C.N.; Worland, A.J. Genetic analysis of some flowering time and adaptive traits in wheat. *New Phytologist.* **1997**, *13*, 19–28. [CrossRef]
68. Lewis, S.; Faricelli, M.E.; Appendino, M.L.; Valárik, M.; Dubcovsky, J. The chromosome region including the earliness per se locus *Eps-A* m1 affects the duration of early developmental phases and spikelet number in diploid wheat. *J. Exp. Bot.* **2008**, *59*, 3595–3607. [CrossRef] [PubMed]
69. Sanchez-Garcia, M.; Bentley, A.R. Global Journeys of Adaptive Wheat Genes. In *Applications of Genetic and Genomic Research in Cereals*, 1st ed.; Miedaner, T., Korzun, V., Eds.; Elsevier Ltd.: Amsterdam, The Netherlands, 2019; pp. 183–200.
70. Iqbal, M.; Navabi, A.; Salmon, D.F.; Yang, R.C.; Murdoch, B.M.; Moore, S.S.; Spaner, D. Genetic analysis of flowering and maturity time in high latitude spring wheat: Genetic analysis of earliness in spring wheat. *Euphytica* **2007**, *154*, 207–218. [CrossRef]
71. Abinasa, M.; Ayana, A.; Bultosa, G. Genetic variability, heritability and trait associations in durum wheat (*Triticum turgidum* L. var. durum) genotypes. *African J. Agric. Res.* **2011**, *6*, 3972–3979. [CrossRef]
72. Seyoum, M.; Alamerew, S.; Bantte, K. Genetic variability, heritability, correlation coefficient and path analysis for yield and yield related traits in upland rice (*Oryza sativa* L.). *J. Plant Sci.* **2012**, *7*, 13–22. [CrossRef]
73. Shrimali, J.; Shekhawat, A.S.; Kumari, S. Genetic variation and heritability studies for yield and yield components in barley genotypes under normal and limited moisture conditions. *J. Pharmacogn. Phytochem.* **2017**, *6*, 233–235.

74. Bilgrami, S.S.; Ramandi, H.D.; Shariati, V.; Razavi, K.; Tavakol, E.; Fakheri, B.A.; Mahdi Nezhad, N.; Ghaderian, M. Detection of genomic regions associated with tiller number in Iranian bread wheat under different water regimes using genome-wide association study. *Sci. Rep.* **2020**, *10*, 1–17. [CrossRef]

75. Berkman, P.J.; Visendi, P.; Lee, H.C.; Stiller, J.; Manoli, S.; Lorenc, M.T.; Lai, K.; Batley, J.; Fleury, D.; Šimková, H.; et al. Dispersion and domestication shaped the genome of bread wheat. *Plant Biotechnol. J.* **2013**, *11*, 564–571. [CrossRef] [PubMed]

76. Edae, E.A.; Bowden, R.L.; Poland, J. Application of population sequencing (POPSEQ) for ordering and imputing genotyping-by-sequencing markers in hexaploid wheat. *G3 Genes Genomes Genet.* **2015**, *5*, 2547–2553. [CrossRef]

77. Rabbi, A.; Hisam, S.M. Genetics of Drought Tolerance in Hard Red Spring Wheat in the Northern United States of America. Ph.D. Thesis, North Dakota State University, Fargo, ND, USA, 2017.

78. Price, A.H.; Tomos, A.D. Genetic dissection of root growth in rice (*Oryza sativa* L.). Ii: Mapping quantitative trait loci using molecular markers. *Theor. Appl. Genet.* **1997**, *95*, 143–152. [CrossRef]

79. Price, A.H.; Steele, K.A.; Moore, B.J.; Barraclough, P.B.; Clark, L.J. A combined RFLP and AFLP linkage map of upland rice (*Oryza sativa* L.) used to identify QTL for root-penetration ability. *Theor. Appl. Genet.* **2000**, *100*, 49–56. [CrossRef]

80. Zhang, Y.M.; Xu, S. Mapping Quantitative Trait Loci in F2 Incorporating Phenotypes of F3 Progeny. *Genetics* **2004**, *166*, 1981–1993. [CrossRef]

81. Stanley, J.D.; Mehring, G.H.; Wiersma, J.J.; Ransom, J.K. A Standardized Method for Determining Tillering Capacity of Wheat Cultivars. *Am. J. Plant Sci.* **2020**, *11*, 604. [CrossRef]

82. Stange, M.; Friedrich Utz, H.; Schrag, T.A.; Melchinger, A.E.; Würschum, T. High-density genotyping: An overkill for QTL mapping? lessons learned from a case study in maize and simulations. *Theor. Appl. Genet.* **2013**, *126*, 2563–2574. [CrossRef]

83. Yi, Q.; Liu, Y.; Zhang, X.; Hou, X.; Zhang, J.; Liu, H.; Hu, Y.; Yu, G.; Huang, Y. Comparative mapping of quantitative trait loci for tassel-related traits of maize in F 2: 3 and RIL populations. *J. Genet.* **2018**, *97*, 253–266. [CrossRef]

84. Mecha, B.; Alamerew, S.; Assefa, A.; Dutamo, D.; Assefa, E. Correlation and path coefficient studies of yield and yield associated traits in bread wheat (*Triticum aestivum* L.) genotypes. *Adv. Plants Agric. Res.* **2017**, *6*, 1–10.

85. Austin, D.F.; Lee, M. Comparative mapping in F2:3 and F6:7 generations of quantitative trait loci for grain yield and yield components in maize. *Theor. Appl. Genet.* **1996**, *92*, 817–826. [CrossRef]

86. Steinfort, U.; Trevaskis, B.; Fukai, S.; Bell, K.L.; Dreccer, M.F. Vernalisation and photoperiod sensitivity in wheat: Impact on canopy development and yield components. *Field Crop. Res.* **2017**, *201*, 108–121. [CrossRef]

87. Sukumaran, S.; Dreisigacker, S.; Lopes, M.; Chavez, P.; Reynolds, M.P. Genome-wide association study for grain yield and related traits in an elite spring wheat population grown in temperate irrigated environments. *Theor. Appl. Genet.* **2015**, *128*, 353–363. [CrossRef]

88. Li, W.L.; Nelson, J.C.; Chu, C.Y.; Shi, L.H.; Huang, S.H.; Liu, D.J. Chromosomal locations and genetic relationships of tiller and spike characters in wheat. *Euphytica* **2002**, *125*, 357–366. [CrossRef]

89. Huang, M.; Mheni, N.; Brown-Guedira, G.; McKendry, A.; Griffey, C.; Van Sanford, D.; Costa, J.; Sneller, C. Genetic analysis of heading date in winter and spring wheat. *Euphytica* **2018**, *214*. [CrossRef]

90. Milner, S.G.; Maccaferri, M.; Huang, B.E.; Mantovani, P.; Massi, A.; Frascaroli, E.; Tuberosa, R.; Salvi, S. A multiparental cross population for mapping QTL for agronomic traits in durum wheat (*Triticum turgidum* ssp. durum). *Plant Biotechnol. J.* **2016**, *14*, 735–748. [CrossRef]

91. Assanga, S.O.; Fuentealba, M.; Zhang, G.; Tan, C.T.; Dhakal, S.; Rudd, J.C.; Ibrahim, A.M.H.; Xue, Q.; Haley, S.; Chen, J.; et al. Mapping of quantitative trait loci for grain yield and its components in a US popular winter wheat TAM 111 using 90K SNPs. *PLoS ONE* **2017**, *12*, 1–21. [CrossRef]

92. Kidane, Y.G.; Gesesse, C.A.; Hailemariam, B.N.; Desta, E.A.; Mengistu, D.K.; Fadda, C.; Mario Enrico, P.; Dell'Acqua, M. A large nested association mapping population for breeding and quantitative trait locus mapping in Ethiopian durum wheat. *Plant Biotechnol. J.* **2019**, *17*, 1380–1393. [CrossRef]

93. Chen, G.F.; Wu, R.G.; Li, D.M.; Yu, H.X.; Deng, Z.; Tian, J.C. Genomewide association study for seeding emergence and tiller number using SNP markers in an elite winter wheat population. *J. Genet.* **2017**, *96*, 177–186. [CrossRef]

94. Kertesz, Z.; Flintham, J.E.; Gale, M.D. Effects of *Rht* dwarfing genes on wheat grain yield and its components under Eastern European conditions. *Cereal Res. Commun.* **1991**, *19*, 297–304.

95. Lanning, S.P.; Martin, J.M.; Stougaard, R.N.; Guillen-Portal, F.R.; Blake, N.K.; Sherman, J.D.; Robbins, A.M.; Kephart, K.D.; Lamb, P.; Carlson, G.R.; et al. Evaluation of near-isogenic lines for three height-reducing genes in hard red spring wheat. *Crop Sci.* **2012**, *52*, 1145–1152. [CrossRef]

96. Sherman, J.D.; Martin, J.M.; Blake, N.K.; Lanning, S.P.; Talbert, L.E. Genetic basis of agronomic differences between a modern and a historical spring wheat cultivar. *Crop Sci.* **2014**, *54*, 1–13. [CrossRef]

97. Zhang, J.; Chen, J.; Chu, C.; Zhao, W.; Wheeler, J.; Souza, E.; Zemetra, R. Genetic Dissection of QTL Associated with Grain Yield in Diverse Environments. *Agronomy* **2014**, *4*, 556–578. [CrossRef]

98. Addison, C.K. Genetic Mapping of Yield and Normalized Difference Vegetative Index in Soft Red Winter Wheat (*Triticum aestivum* L.). Master's Thesis, University of Arkansas, Fayetteville, NC, USA, 2015.

99. Colebrook, E.H.; Thomas, S.G.; Phillips, A.L.; Hedden, P. The role of gibberellin signalling in plant responses to abiotic stress. *J. Exp. Biol.* **2014**, *217*, 67–75. [CrossRef]

100. Van De Velde, K.; Ruelens, P.; Geuten, K.; Rohde, A.; Van Der Straeten, D. Exploiting DELLA Signaling in Cereals. *Trends Plant Sci.* **2017**, *22*, 880–893. [CrossRef]

101. Jia, Q.J.; Zhang, J.J.; Westcott, S.; Zhang, X.Q.; Bellgard, M.; Lance, R.; Li, C.D. *GA-20* oxidase as a candidate for the semidwarf gene *sdw1/denso* in barley. *Funct. Integr. Genomics* **2009**, *9*, 255–262. [CrossRef]

102. Jia, Q.; Zhang, X.Q.; Westcott, S.; Broughton, S.; Cakir, M.; Yang, J.; Lance, R.; Li, C. Expression level of a gibberellin *20-oxidase* gene is associated with multiple agronomic and quality traits in barley. *Theor. Appl. Genet.* **2011**, *122*, 1451–1460. [CrossRef]

103. Jia, Q.; Li, C.; Shang, Y.; Zhu, J.; Hua, W.; Wang, J.; Yang, J.; Zhang, G. Molecular characterization and functional analysis of barley semi-dwarf mutant Riso no. 9265. *BMC Genomics* **2015**, *16*, 1–11. [CrossRef]

104. Kuczyńska, A.; Mikołajczak, K.; Ćwiek, H. Pleiotropic effects of the sdw1 locus in barley populations representing different rounds of recombination. Electron. *J. Biotechnol.* **2014**, *17*, 217–223. [CrossRef]

105. Tan, L.; Li, X.; Liu, F.; Sun, X.; Li, C.; Zhu, Z.; Fu, Y.; Cai, H.; Wang, X.; Xie, D.; et al. Control of a key transition from prostrate to erect growth in rice domestication. *Nat. Genet.* **2008**, *40*, 1360–1364. [CrossRef]

106. Chen, X.; Lu, S.; Wang, Y.; Zhang, X.; Lv, B.; Luo, L.; Xi, D.; Shen, J.; Ma, H.; Ming, F. OsNAC2 encoding a NAC transcription factor that affects plant height through mediating the gibberellic acid pathway in rice. *Plant J.* **2015**, *82*, 302–314. [CrossRef]

107. Mao, C.; Ding, W.; Wu, Y.; Yu, J.; He, X.; Shou, H.; Wu, P. Overexpression of a NAC-domain protein promotes shoot branching in rice. *New Phytol.* **2007**, *176*, 288–298. [CrossRef]

108. Zhou, X.; Zhang, Z.L.; Park, J.; Tyler, L.; Yusuke, J.; Qiu, K.; Nam, E.A.; Lumba, S.; Desveaux, D.; McCourt, P.; et al. The ERF11 transcription factor promotes internode elongation by activating gibberellin biosynthesis and signaling. *Plant Physiol.* **2016**, *171*, 2760–2770. [CrossRef]

109. Sakuraba, Y.; Kim, E.Y.; Paek, N.C. Roles of rice PHYTOCHROME-INTERACTING FACTOR-LIKE1 (OsPIL1) in leaf senescence. *Plant Signal. Behav.* **2017**, *12*, 3–7. [CrossRef]

110. Franklin, K.A.; Lee, S.H.; Patel, D.; Kumar, S.V.; Spartz, A.K.; Gu, C.; Ye, S.; Yu, P.; Breen, G.; Cohen, J.D.; et al. Phytochrome-Interacting Factor 4 (PIF4) regulates auxin biosynthesis at high temperature. *Proc. Natl. Acad. Sci. USA* **2011**, *108*, 20231–20235. [CrossRef]

111. Bahuguna, R.N.; Jagadish, K.S.V. Temperature regulation of plant phenological development. *Environ. Exp. Bot.* **2015**, *111*, 83–90. [CrossRef]

112. Cao, X.; Yang, H.; Shang, C.; Ma, S.; Liu, L.; Cheng, J. The roles of auxin biosynthesis YUCCA gene family in plants. *Int. J. Mol. Sci.* **2019**, *20*, 6343. [CrossRef] [PubMed]

113. Wahl, V.; Ponnu, J.; Schlereth, A.; Arrivault, S.; Langenecker, T.; Franke, A.; Feil, R.; Lunn, J.E.; Scitt, M.; Schmid, M. Regulation of flowering by trehalose-6-phosphate signaling in *Arabidopsis thaliana*. *Science* **2013**, *339*, 704–707. [CrossRef]

114. Fichtner, F.; Olas, J.J.; Feil, R.; Watanabe, M.; Krause, U.; Hoefgen, R.; Stitt, M.; Lunn, J.E. Functional features of TREHALOSE-6-PHOSPHATE SYNTHASE1, an essential enzyme in *Arabidopsis*. *Plant Cell* **2020**, *32*, 1949–1972. [CrossRef]

115. Sun, J.; Gibson, K.M.; Kiirats, O.; Okita, T.W.; Edwards, G.E. Interactions of nitrate and CO_2 enrichment on growth, carbohydrates, and rubisco in *Arabidopsis* starch mutants. Significance of starch and hexose. *Plant Physiol.* **2002**, *130*, 1573–1583. [CrossRef]

116. Sato, S.; Yanagisawa, S. Characterization of metabolic states of *Arabidopsis thaliana* under diverse carbon and nitrogen nutrient conditions via targeted metabolomic analysis. *Plant Cell Physiol.* **2014**, *55*, 306–319. [CrossRef]